Differential actin binding along the PEVK domain of skeletal muscle titin

Attila Nagy[1], Paola Cacciafesta[1,*], László Grama[1], András Kengyel[1], András Málnási-Csizmadia[2] and Miklós S. Z. Kellermayer[1,‡]

[1]Department of Biophysics, University of Pécs, Faculty of Medicine, Szigeti út 12. Pécs 7624, Hungary
[2]Department of Biochemistry, Eötvös University, Pázmány Péter sétány 1/c., Budapest 1117, Hungary
*Present address: Universita' degli Studi di Firenze, LENS, via Nello Carrara 1, 50019 Sesto Fiorentino (Firenze), Italy
‡Author for correspondence (e-mail: miklos.kellermayer.jr@aok.pte.hu)

Accepted 18 August 2004
Journal of Cell Science 117, 5781-5789 Published by The Company of Biologists 2004
doi:10.1242/jcs.01501

Summary

Parts of the PEVK (Pro-Glu-Val-Lys) domain of the skeletal muscle isoform of the giant intrasarcomeric protein titin have been shown to bind F-actin. However, the mechanisms and physiological function of this are poorly understood. To test for actin binding along PEVK, we expressed contiguous N-terminal (PEVKI), middle (PEVKII), and C-terminal (PEVKIII) PEVK segments of the human soleus muscle isoform. We found a differential actin binding along PEVK in solid-state binding, cross-linking and in vitro motility assays. The order of apparent affinity is PEVKII>PEVKI>PEVKIII. To explore which sequence motifs convey the actin-binding property, we cloned and expressed PEVK fragments with different motif structure: PPAK, polyE-rich and pure polyE fragments. The polyE-containing fragments had a stronger apparent actin binding, suggesting that a local preponderance of polyE motifs conveys an enhanced local actin-binding property to PEVK. The actin binding of PEVK may serve as a viscous bumper mechanism that limits the velocity of unloaded muscle shortening towards short sarcomere lengths. Variations in the motif structure of PEVK might be a method of regulating the magnitude of the viscous drag.

Key words: Titin, PEVK, PPAK, polyE, In vitro motility, Elasticity

Introduction

One of the main determinants of muscle elasticity is the filamentous intrasarcomeric protein titin, also called connectin (Wang et al., 1979; Maruyama, 1997), a 3.0-3.7 MDa protein that spans the half sarcomere (for recent reviews, see Granzier and Labeit, 2004; Miller et al., 2004; Tskhovrebova and Trinick, 2003). Titin is anchored to the Z- and M-lines and is attached to the thick filaments of the A-band (Fürst et al., 1988). The I-band section of the molecule is constructed of serially linked immunoglobulin (Ig)-like domains (proximal and distal tandem Ig regions) interspersed with unique sequences including a proline-, glutamate-, valine- and lysine-rich (PEVK) domain (Labeit and Kolmerer, 1995). When stretching the sarcomere, a passive force is generated by the extension of the I-band section of titin. The extension of this I-band section occurs as a series of consecutive events (Gautel and Goulding, 1996): the extension of the tandem Ig segment is followed by the extension of the PEVK domain (Linke et al., 1996; Trombitás et al., 1998) and by the N2-B unique sequence in cardiac muscle (Helmes et al., 1999; Linke et al., 1999). Titin isoforms of different lengths are expressed in different muscle types (Freiburg et al., 2000; Labeit and Kolmerer, 1995). Cardiac muscle contains the shortest titin isoform (N2B) with a 163-residue-long PEVK domain (Freiburg et al., 2000; Labeit and Kolmerer, 1995). By contrast, in soleus muscle the PEVK segment is 2174 residues in length (Freiburg et al., 2000; Labeit and Kolmerer, 1995).

The PEVK domain of titin has been suggested to acquire a random structure owing to the preponderance of highly charged residues (Labeit and Kolmerer, 1995). Indeed, early immunoelectron microscopic analysis has shown that the PEVK domain probably behaves as a quasi-unfolded, random protein chain (Trombitás et al., 1998). Recent structural experiments suggest that the PEVK domain may contain left-handed polyproline helices (Ma et al., 2001). Furthermore, a repetitive motif structure of PEVK has been demonstrated based on sequence analysis (Greaser, 2001). Two main motifs were identified in the PEVK sequence: (1) PPAK and (2) polyE motifs. The PPAK motifs are ~28-residue-long sequences which begin most often with the amino acids PPAK. PolyE motifs contain a preponderance of glutamate. Based on NMR and CD spectroscopic data, Ma and Wang recently suggested that the PEVK domain has a malleable structure which is capable of transition between various conformational states: polyproline helix, beta turn and unordered coil (Ma and Wang, 2003).

Titin has been shown previously to bind actin (Kellermayer and Granzier, 1996; Maruyama et al., 1987; Soteriou et al., 1993). Several different segments or elements of the molecule were demonstrated to possess independent actin-binding properties. Near the Z-line, titin is tightly associated with a 100-nm-long stretch of the thin filament (Trombitás and Granzier, 1997). A group of globular domains from the A-band super-repeat region show actin-binding properties, but the physiological significance of this is unclear (Jin, 1995). The PEVK domain of cardiac titin binds F-actin in a Ca^{2+}/S100-

regulated manner (Yamasaki et al., 2001) and an interaction between cardiac PEVK and F-actin has also been demonstrated (Kulke et al., 2001; Linke et al., 2002). A C-terminal PEVK fragment of the skeletal muscle titin binds actin but with a lower apparent affinity than cardiac N2B PEVK (Linke et al., 2002). Notably, the cardiac titin sequence is inclusive in the skeletal isoform, therefore there might be regional differences in the actin binding of skeletal PEVK. The exact mechanisms of PEVK-actin binding and its physiological significance are largely unknown.

In the present work we explored actin binding along skeletal PEVK by applying a multi-faceted approach: heterologous expression of various skeletal PEVK segments and fragments, in vitro motility assays, solid-state and co-sedimentation binding assays, fluorescent protein modification and fluorescence imaging. We found that the PEVK domain binds F-actin along its entire length, but with different apparent local affinities. The apparent binding strength increases with poly-E motif content, suggesting that this sequence element is primarily responsible for conveying the actin-binding property. PEVK-actin binding reduces the sliding velocity in the in vitro motility assay; such a process may also occur in the sarcomere, where actin-PEVK interaction may play a role in regulating the velocity of unloaded muscle shortening.

Materials and Methods

Cloning, expression and purification of human skeletal PEVK

Human skeletal muscle cDNA library was a generous gift of Dr Siegfried Labeit. The entire skeletal PEVK domain (largest, m. soleus isoform) was expressed in three contiguous segments, each corresponding to approximately one third (~700 residues) of the PEVK length: N-terminal (PEVKI), middle (PEVKII) and C-terminal (PEVKIII). The nucleotide sequence boundaries of the PEVK segments, based on GenBank accession no. X90569 (version X90569.1) (Labeit and Kolmerer, 1995) are as follows: PEVKI 16852-19074 (amino acids 5618-6358), PEVKII 19075-21192 (6359-7064) and PEVKIII 21193-23373 (7065-7791). A 151-residue-long polyE-rich and a 201-residue-long PPAK were also cloned and expressed, and their boundaries were the following: PPAK 17413-18015 (amino acids 5805-6005), polyE-rich 20305-20757 (6769-6919). In addition, a 146-residue-long 'pure polyE' fragment was designed, cloned and expressed from a tandem doublet of the following sequence: 20305-20520 (amino acids 6769-6840). This fragment was cloned in two consecutive steps into pET-28a vector between *Nhe*I-*Eco*RI and *Eco*RI-*Xho*I sites. As a result, the expressed protein contained two extra amino acid residues (E and F) between the two tandem sequences. In the present work, we denote PEVKI, II and III as 'PEVK segments', whereas the PPAK, polyE-rich and pure polyE sequences are termed 'PEVK fragments'. The arrangement of PEVK segments and fragments along skeletal PEVK is shown in Fig. 1A. Each of the segments and fragments was cloned into pET-28a vector (Novagen) between *Nhe*I and *Xho*I sites introduced independently with PCR by using specific oligonucleotides. To the C-terminus of the recombinant proteins, two vicinal cysteines were added for subsequent fluorescent modification. Proteins were expressed in *E. coli* BL21(DE3)pLysS. His_6-tagged (on N-terminus) proteins were purified on Ni^{2+}-NTA columns under native conditions following manufacturer's instructions (Qiagen) and further purified on a Sephadex G-25 column. Concentrations were determined with Bradford reagent (Sigma). (As Bradford reagent binds to basic and aromatic residues, the concentration of PPAK and polyE fragments may have been slightly over- and underestimated, respectively.) As shown by the gel profile of the purified PEVK segments and fragments (Fig. 1B), the protein samples were of high purity and devoid of degradation products.

Preparation of proteins

Actin (Pardee and Spudich, 1982), myosin (Margossian and Lowey, 1982) and heavy meromyosin (HMM) (Kron et al., 1991) were purified according to established methods. F-actin was fluorescently labelled with molar excess of tetramethylrhodamine-isothiocyanate-phalloidin (TRITC-phalloidin, Molecular Probes). Tropomyosin was a kind gift from Emöke Bódis. Native thin filaments were prepared from glycerinated rabbit papillary muscles using published protocols (Knight and Lovell, 1982) with modifications. Briefly, glycerinated rabbit left ventricular papillary muscles were homogenized, washed with rigor buffer (25 mM MOPS pH 7.4, 100 mM KCl, 4 mM $MgCl_2$, 1 mM EGTA, 1 mM DTT) in successive sedimentation resuspension cycles (2000 ***g***, 5 minutes, 4°C) and then labeled with TRITC-phalloidin. Myofibrils were partially digested with chymotrypsin (chymotrypsin/myofibril ratio 10 μg/1mg) for 10 minutes at 25°C. The reaction was stopped by adding excess PMSF in ice-cold solution. Subsequently the sample was centrifuged (Sorvall OTD80; 80,000 ***g***, 30 minutes, 4°C) to remove debris. The supernatant was analyzed for protein composition and used in the in vitro motility assay.

In vitro motility assay

The in vitro motility assay was carried out according to published protocols (Kellermayer and Granzier, 1996; Kellermayer et al., 1995; Kron et al., 1991). The flow-through microchamber used had an internal volume of ~10 μl (Kellermayer, 1997; Kellermayer and Granzier, 1996). First, 10 μl of HMM-PEVK mixture in assay buffer (25 mM imidazole-HCl, 25 mM KCl, 4 mM $MgCl_2$, 1 mM EGTA, 1 mM DTT, pH 7.4) was pipetted through the microchamber and

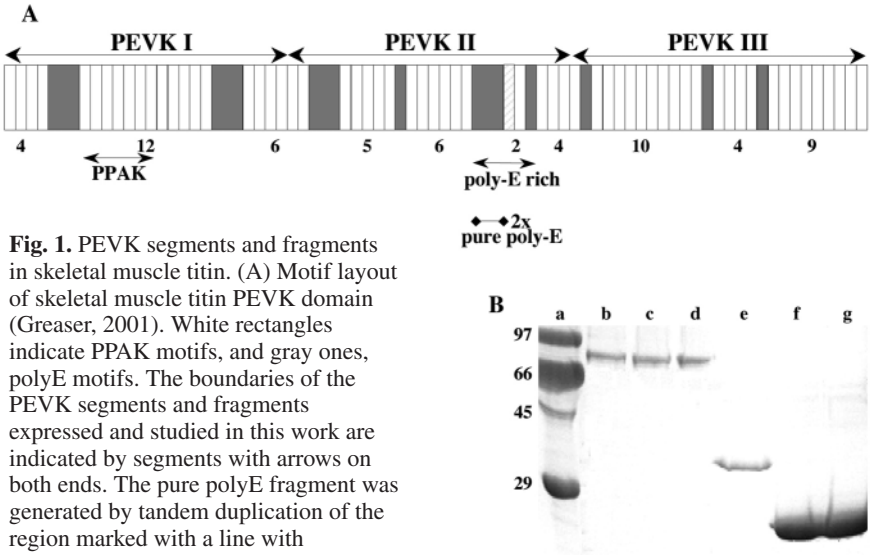

Fig. 1. PEVK segments and fragments in skeletal muscle titin. (A) Motif layout of skeletal muscle titin PEVK domain (Greaser, 2001). White rectangles indicate PPAK motifs, and gray ones, polyE motifs. The boundaries of the PEVK segments and fragments expressed and studied in this work are indicated by segments with arrows on both ends. The pure polyE fragment was generated by tandem duplication of the region marked with a line with diamonds at both ends. (B) SDS-PAGE of the expressed and purified PEVK segments and fragments. (a) molecular weight standards, (b) PEVKI, (c) PEVKII, (d) PEVKIII, (e) PPAK, (f) polyE-rich and (g) pure polyE.

incubated at room temperature for 1 minute. An HMM concentration of 40 μg/ml was used throughout the different experiments and the PEVK concentration was adjusted to obtain different PEVK/HMM molar ratios. The motility assays were carried out with the assumption that the surface binding of either HMM or PEVK is not significantly influenced by the their mutual presence, therefore the solution molar ratios correspond to the relative surface densities (Kellermayer and Granzier, 1996). Nonspecific binding sites were blocked by washing in 100 μl 0.5 mg/ml BSA in assay buffer. Actin filaments were added at a concentration of 70 ng/ml and allowed to bind to the HMM-PEVK-coated surface for 1 minute. The flow-cell was then washed with 100 μl assay buffer supplemented with an oxygen scavenger enzyme system (6 mg/ml D-glucose, 40 μg/ml catalase, 200 μg/ml glucose oxidase) (Harada et al., 1987) and 100 mM β-mercaptoethanol to reduce photobleaching. Filament movement was initiated by the infusion of 1 mM ATP and the motility assay was carried out at 30°C. For high ionic strength (140 mM KCl) experiments, the in vitro motility assay was carried out in the presence of 1% methylcellulose (Sigma M0512) to reduce the lateral Brownian movement of actin filaments. Filament velocity was measured on digitized video sequences (usually 30 frames) by user-developed Pascal algorithms. The typical time between the digitized frames was 0.2 sec. The mean velocity was calculated for all filaments in a field of view.

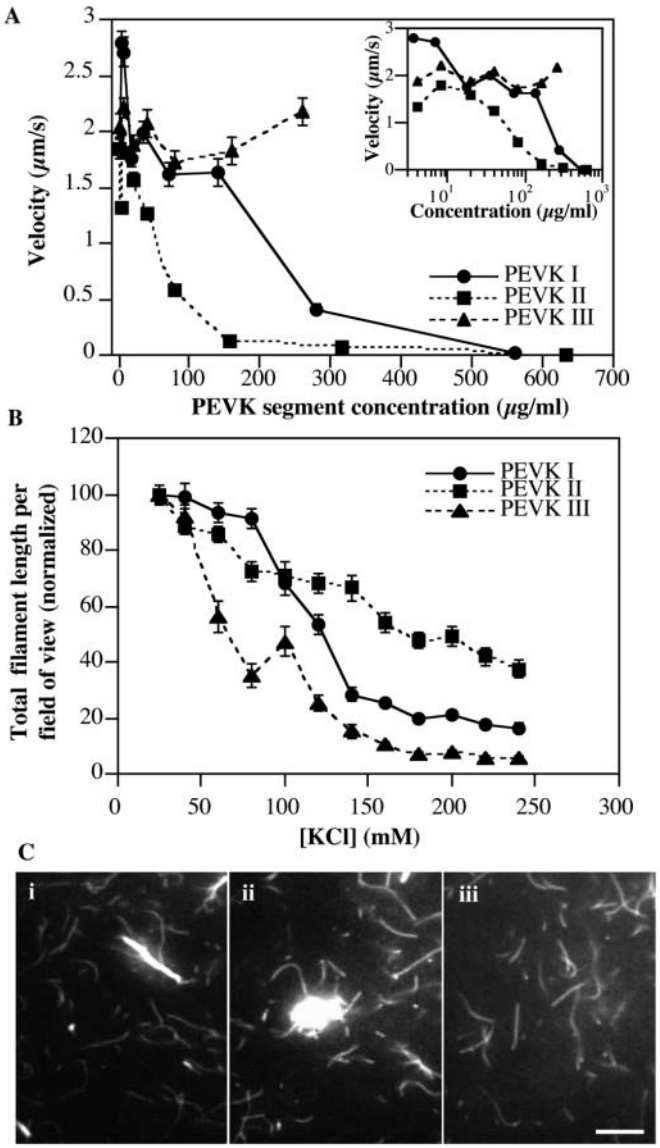

Fig. 2. Interaction of PEVK segments with actin. (A) Effect of PEVK segments on in vitro acto-HMM motility. Velocity as a function of PEVKI, -II and -III segment concentration. Inset graph shows velocity as a function of log[PEVK segment]. The in vitro motility assay was carried out at a KCl concentration of 25 mM, HMM concentration of 40 μg/ml and ATP concentration of 1 mM. (B) Solid-state surface binding of F-actin by PEVK segments as a function of ionic strength (adjusted by varying KCl concentration). The total filament length per field of view at the initial concentration of 25 mM KCl, were 115 μm, 145 μm and 195 μm for the PEVKI, -II and -III segments, respectively. (C) Actin crosslinking assay with various PEVK fragments (i) PEVKI, (ii) PEVKII and (iii) PEVKIII. Bar, 20 μm.

Solid-state surface binding assay

Interaction between PEVK segments or fragments and actin filaments was studied in an in vitro microscopic binding assay essentially according to previously reported steps (Kellermayer and Granzier, 1996). Briefly, the amount of actin bound to a PEVK-coated nitrocellulose surface was assessed by measuring the total filament length per field of view. First, PEVK was added to the microchamber and allowed to bind to the nitrocellulose surface for 1 minute. Nonspecific binding sites were then blocked with 0.5 mg/ml BSA in assay buffer. Fluorescently labeled actin filaments (70 ng/ml) were added and allowed to bind to the PEVK-coated surface for 1 minute. Unbound filaments were washed away with assay buffer supplemented with the oxygen-scavenger enzyme system (see above). Filament length was measured by using a user-developed macro program that automatically traced filaments and measured their length in a sequence of digitized images. Because the algorithm treats single and crosslinked filaments (that run parallel) equally, surface-bound actin quantity is underestimated in the case of extensive filament crosslinking. Ionic strength was adjusted by washing in solution containing progressively increasing concentrations of KCl. For calcium-dependent binding assays, pCa was calculated by the computer program of Fabiato (Fabiato, 1988) and adjusted by adding $CaCl_2$.

Actin crosslinking assay

The actin filament crosslinking effect of PEVK segments or fragments was measured by visualizing fluorescently labeled actin filaments. PEVK (final concentration 2.5 μM) was mixed with TRITC-phalloidin-labeled F-actin (final concentration 0.3 μM) in assay buffer containing 140 mM KCl and incubated at room temperature for 5 minutes. The mixture was complemented with an oxygen-scavenger enzyme system (see above), and an aliquot was visualized in either an epifluorescence (Zeiss) or total internal reflection fluorescence microscope (TIRFM, Olympus). The extent of F-actin crosslinking was estimated by counting the crosslinked actin aggregates per field of view. An object was considered an aggregate if its fluorescence intensity and dimensions exceeded those of the single actin filament at least threefold.

Actin-PEVK co-sedimentation assay

Phalloidin-labeled F-actin (2 μM) and skeletal PEVK fragments were incubated with 140 mM KCl, 25 mM imidazole, 4 mM $MgCl_2$, 1 mM EGTA, 1 mM DTT at room temperature for 10 minutes. Samples were centrifuged at 100,000 ***g*** for 60 minutes then separated by SDS-polyacrylamide gel electrophoresis (12%) (Laemmli, 1970). Gels were stained with Coomassie Brilliant Blue R-250, then imaged, digitized and analyzed with a Syngene MultiGenius Bio Imaging system using GeneSnap and GeneTools software. Protein quantities were calculated by integrating the grayscale densities of the bands corrected for specific Coomassie binding measured in independent calibration experiments.

Preparation, labeling and imaging of myofibrils

PEVKII segment was labeled on the C-terminal cysteine residues (added during the cloning steps) by incubating overnight in the presence of 10× molar excess of iodoacetamido fluorescein (IAF, Molecular Probes). Myofibrils were prepared from glycerinated rabbit psoas muscle by using previously published protocols (Knight and Trinick, 1982). Briefly, glycerinated muscle bundles, stored in 50% glycerol at –20°C, were homogenized in rigor buffer (see above) on ice, washed by successive cycles of sedimentation (2000 ***g***, 5 minutes, 4°C) and resuspension in rigor buffer. A 5-μl sample was placed on a glass coverslip. Unbound myofibrils were washed away with rigor buffer. IAF-labeled PEVKII (0.1 mg/ml) was allowed to bind at room temperature for 15 minutes. Unbound PEVKII was washed away with five washes of rigor buffer. Myofibrils were visualized in a laser-scanning confocal microscope (Bio-Rad MRC 1024 attached to a Nikon Eclipse inverted microscope) using a 40× phase objective lens (0.75 N.A., Nikon Plan Fluor). The 488-nm line of an Argon ion laser (120-360 μW) was used. Fluorescence and phase-contrast images were simultaneously acquired. Alternatively, fluorescence microscopic images were collected in an epifluorescence (Zeiss) or TIRF (Olympus) microscope.

Steady-state actin-activated ATPase measurements

Steady-state ATPase activity of HMM was measured by using an NADH (nicotinamide adenine dinucleotide, reduced) coupled assay at 25°C in a buffer containing 10 mM MOPS (pH 7.0), 2 mM $MgCl_2$, 0.15 mM EGTA, 1 mM ATP, 40 U/ml lactate dehydrogenase (LDH), 200 U/ml pyruvate kinase, 1 mM phosphoenolpyruvate (PEP) and 200 μM NADH. Protein concentrations were: 0.2 μM HMM, 20 μM actin, 2.3-23 μM PPAK fragment and 2.9-29 μM polyE fragment. Changes in A_{340} (ε_{340}=6220 $M^{-1}cm^{-1}$) as a function of time were followed using a Jasco V-550 UV-VIS spectrophotometer.

Results

Inhibition of in vitro acto-HMM motility by PEVK

The effect of PEVKI, -II and -III on acto-HMM motility was studied using the in vitro motility assay (Fig. 2A). The addition of PEVKI and -II resulted in reduced actin filament velocities. Velocity decreased with increasing concentration of added PEVK segment. The greatest degree of motility inhibition was observed in the case of PEVKII. By contrast, essentially no inhibition was observed in the case of PEVKIII in the concentration range studied. The movement of actin filaments in the presence of either PEVKI or -II was not smooth, but often bursts of movement interrupted stationary periods, which resulted in a ‘stop-and-go’ motion. To test whether the motility inhibition might be due to interference of the PEVK segments with the HMM ATPase, we measured the actin-activated ATPase activity of HMM in the presence of the segments. None of the segments inhibited the ATPase activity (data not shown).

Solid-state surface binding assay

To examine the binding of F-actin to PEVK segments, we first carried out solid-state surface binding assays, where actin filaments were allowed to bind to a surface coated with PEVK segment. To explore binding mechanisms and estimate the strength of actin binding, the ionic strength was increased by increasing KCl concentration. Actin filaments gradually dissociated from the PEVK segment-covered surface upon increasing the KCl concentration. The surface density of F-actin, measured for PEVKI, -II and -III as the total actin filament length per field of view, as a function of KCl concentration is shown in Fig. 2B. The strongest apparent actin binding, i.e. lowest tendency for actin dissociation with increasing KCl concentration, was observed in the case of PEVKII. The weakest binding was observed with PEVKIII.

Crosslinking of actin filaments by PEVK

To examine the actin crosslinking effect of the PEVK segments, actin filaments and the respective PEVK segment were mixed in solution (Fig. 2C). Actin bundles were observed

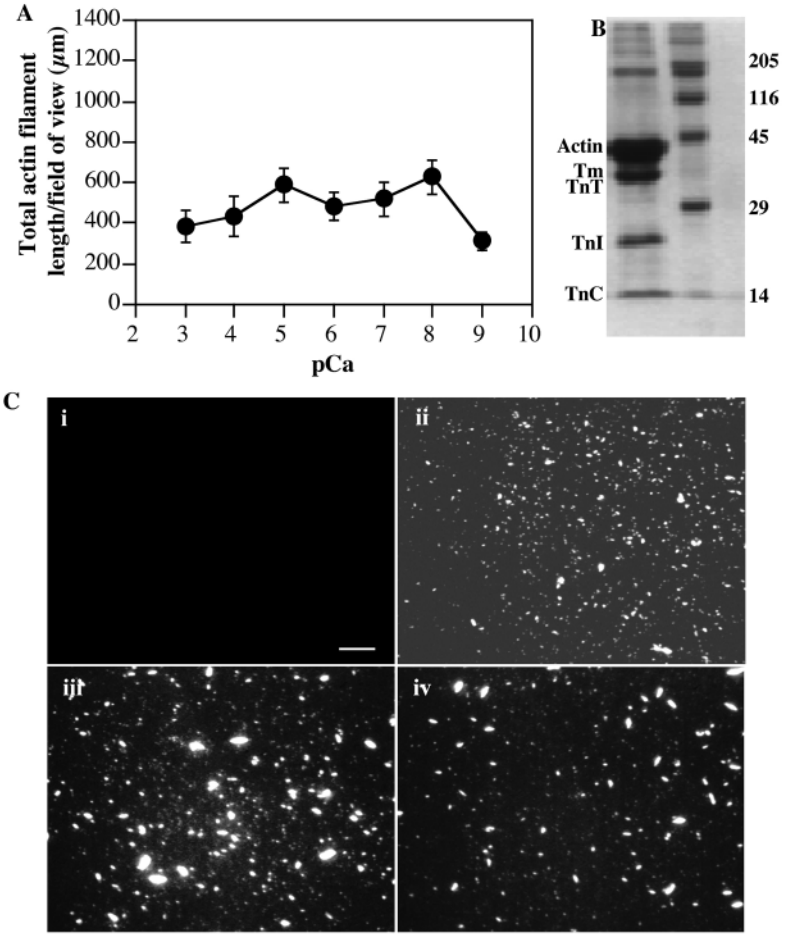

Fig. 3. Effect of calcium and Ca^{2+} regulatory proteins on the actin binding of PEVKII. (A) Solid-state surface binding of F-actin by PEVKII as a function of free Ca^{2+} concentration (pCa). (B) SDS-PAGE of isolated native thin filaments. Left lane, thin filament preparation; right lane, molecular weight standards. Tm, tropomyosin; TnT, troponin T; TnI, troponin I; TnC, troponin C. (C) Surface binding of native thin filaments by PEVKII. Only short filaments are observed, in accordance with the size of the native thin filaments (~1 μm). (i) Negative control (BSA on the surface). (ii) Positive control (HMM-coated surface; pCa 3). (iii) PEVKII-coated surface; pCa 9. (iv) PEVKII-coated surface; pCa 3. Bar, 10 μm.

in the case of PEVKI (Fig. 2Ci) and -II (Fig. 2Cii). In some cases huge bundles up to 20-30 μm in length and 5 μm in width were observed. Negligible actin crosslinking was seen in the case of PEVKIII (Fig. 2Ciii).

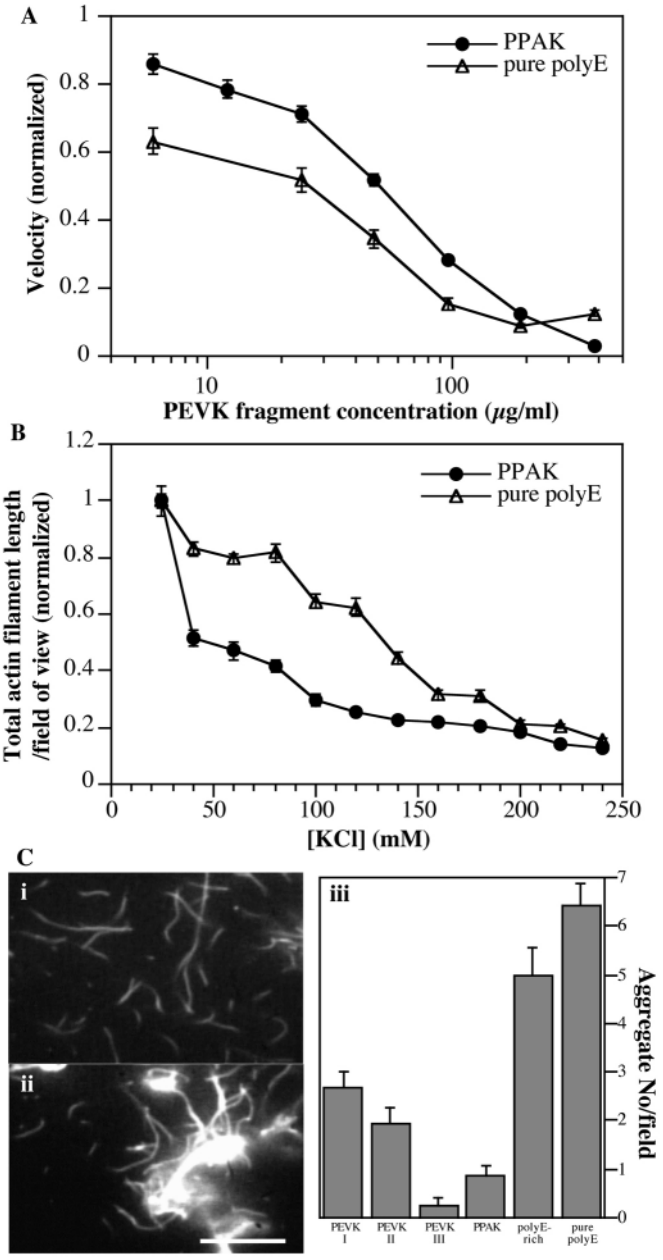

Fig. 4. Interaction of various PEVK fragments with actin. (A) In vitro acto-HMM velocity as a function of PPAK and pure polyE fragment concentration. The assay was carried out in the presence of 140 mM KCl. The data were normalized to the velocity in the absence of PEVK fragment (concentration=0 μg/ml), which was 3.2 μm/s for the PPAK fragment and 3.0 μm/s for the pure polyE fragment. (B) Solid-state surface binding of F-actin by PPAK and pure polyE fragments as a function of KCl concentration. The total filament length per field of view at the initial concentration of 25 mM KCl were 400 μm and 1140 μm for the PPAK and pure polyE fragments, respectively. (C) F-actin crosslinking assay in the presence of various PEVK fragments. (i) Actin filaments in the presence of PPAK. (ii) Crosslinked actin filaments in the presence of pure polyE fragment. Bar 20 μm. (iii) Summary of the actin-crosslinking assay.

Effect of Ca^{2+} and Calcium regulatory proteins on PEVK-actin binding

To test the effect of Ca^{2+} on the F-actin binding by PEVK, we measured the solid-state F-actin binding by surface-adsorbed PEVKII (Fig. 3A). Across a pCa range of 3-9 we found no significant difference in the F-actin binding by PEVKII. To investigate the effect of the presence of calcium regulatory proteins on PEVK-actin interaction, we measured the solid-state binding of native thin filaments by surface-adsorbed PEVKII (Fig. 3B,C). Native thin filaments bound to surface-adsorbed PEVKII in significant quantities at pCa values of 3-9, suggesting that neither Ca^{2+}, nor calcium regulatory proteins significantly influence the actin-binding properties of PEVKII, or the PEVKII-binding properties of F-actin. We also observed that PEVKII was able to crosslink synthetic thin filaments reconstituted from F-actin and purified tropomyosin (data not shown).

Interaction between PPAK, polyE-rich and pure polyE PEVK fragments with F-actin

To investigate which motifs are primarily responsible for the actin-binding properties of PEVK, we expressed PEVK fragments that correspond to the motif elements of PEVK (Greaser, 2001) (Fig. 1A). Initial analysis of the motif structure of skeletal PEVK suggested that a local preponderance of polyE motifs might convey a local actin-binding feature, considering that PEVKII, which is the richest in polyE motifs,

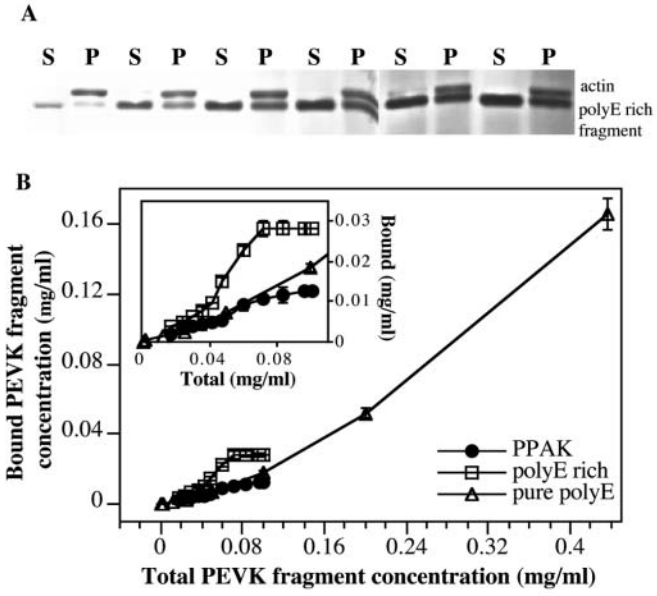

Fig. 5. PEVK fragment–F-actin co-sedimentation assay. (A) SDS-PAGE of polyE-rich fragment-actin binding assay. S, supernatant; P, pellet. The total polyE concentrations for the S-P lane pairs in this assay were: 0.036, 0.048, 0.060, 0.072, 0.084 and 0.096 mg/ml from left to right of gel. (B) Bound PEVK fragment concentration as a function of total PEVK fragment concentration. Inset shows a magnified view of the low-concentration range.

demonstrated the greatest degree of apparent actin binding. The interaction of the various PEVK fragments with F-actin was studied with in vitro motility (Fig. 4A) and surface binding (Fig. 4B), actin crosslinking (Fig. 4C) and co-sedimentation (Fig. 5) assays. In vitro motility was inhibited by each PEVK fragment. The results for PPAK and pure polyE are shown in Fig. 4A. The results indicate that the pure polyE fragment exerts a greater inhibitory effect on in vitro motility than PPAK. To test whether the motility inhibition might be due to interference of the PEVK fragments with the HMM ATPase, we measured the actin-activated ATPase activity of HMM. None of the fragments inhibited the ATPase activity. In solid-state surface actin-binding assays, the pure polyE fragment bound F-actin with a greater apparent affinity than the PPAK fragment (Fig. 4B). Crosslinked F-actin aggregates were observed in the case of each PEVK fragment, but were most prominent in the case of the pure polyE fragment (Fig. 4Ci and ii). Based on the number of aggregates per field of view, the extent of actin crosslinking was greater in the case of the polyE-rich and pure polyE fragments than in the case of the PPAK fragment. The results of the F-actin crosslinking assay are summarized in Fig. 4Ciii. In PEVK fragment-F-actin co-sedimentation assays a more pronounced actin binding was observed in the case of pure polyE and polyE-rich fragments than the PPAK fragment (Fig. 5). In the case of the pure polyE fragment, we were unable to reach a large enough polyE:actin ratio experimentally to observe saturation. Scatchard plots (data not shown) and preliminary stopped flow kinetics measurements indicate that the binding mechanisms differ from a canonical binding between a macromolecule and ligand, where independent and identical binding sites are involved.

Binding of PEVK to myofibrils

To examine whether PEVK binds to actin in situ in the sarcomere, we incubated purified rabbit psoas myofibrils with a fluorescently (IAF) labeled PEVKII fragment and observed the distribution of fluorescence by using laser-scanning confocal microscopy. The phase-contrast and the corresponding fluorescence microscopic images of a myofibril are shown in Fig. 6A. The relatively low overall fluorescence intensity may be attributed to several factors including the size and shape of the externally added PEVKII segment, its low labeling efficiency and particularly spatial constraints against the diffusion of the segment into the sarcomeric lattice. Regions of high fluorescence coincide with the I-band of the sarcomere, indicating that PEVKII did bind to the thin filaments (Fig. 6B). The length of the fluorescent region along the myofibril axis is somewhat smaller than the I-band width, suggesting that the entire length of the thin filaments is not fully accessible to PEVKII binding. Interestingly, the Z-line shows high fluorescence intensity, pointing to the possibility that PEVKII binds to the Z-line. The implication of PEVK binding in the Z-line is, as yet, unclear. It is also unclear how PEVK segments other than the one used here from soleus muscle would bind within the sarcomere.

Discussion

The interaction between F-actin and the PEVK domain of the skeletal muscle titin isoform was studied in this work. It has been previously shown that the PEVK domain of N2B cardiac titin binds F-actin (Kulke et al., 2001; Linke et al., 1997; Linke et al., 2002; Yamasaki et al., 2001). Furthermore, there has been a recent report that a C-terminal skeletal PEVK fragment, which contains the constitutively-expressed N2B cardiac PEVK sequence, also binds F-actin, but with smaller affinity than the cardiac isoform (Linke et al., 2002). Considering that actin-PEVK interaction might play a regulatory role in muscle contraction, a detailed analysis of actin-PEVK binding is important. Here we systematically analyzed the actin-binding property along the skeletal PEVK domain by expressing an N-terminal (PEVKI), middle (PEVKII) and C-terminal (PEVKIII) one-third of the domain. The segments bound F-actin differently, suggesting that there is a differential actin binding along the skeletal PEVK domain. The actin-binding property of the various PEVK segments was manifested in several distinct results: PEVK segments (1) inhibited in vitro acto-HMM motility by tethering actin filaments to the surface; (2) bound actin filaments in surface binding assays; (3) bound actin filaments in co-sedimentation assays; (4) crosslinked actin filaments; and (5) bound to the I-band region of the skeletal muscle sarcomere. To explore which of the PPAK or polyE motif elements convey the actin-binding property, we cloned and

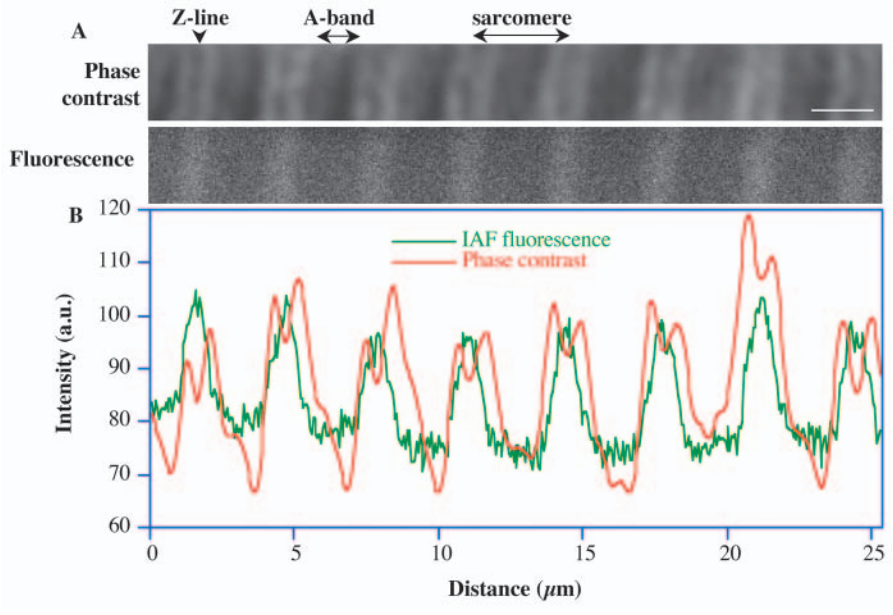

Fig. 6. Binding of IAF-labeled PEVKII to purified rabbit psoas myofibrils. (A) Confocal microscopic images of a myofibril incubated with a fluorescently labeled PEVKII segment. Phase-contrast (upper panel) and the corresponding fluorescence (lower panel) microscopic images are shown. Bar, 2 μm. (B) Grayscale intensity along the myofibril axis for both the phase contrast and fluorescence microscopic images.

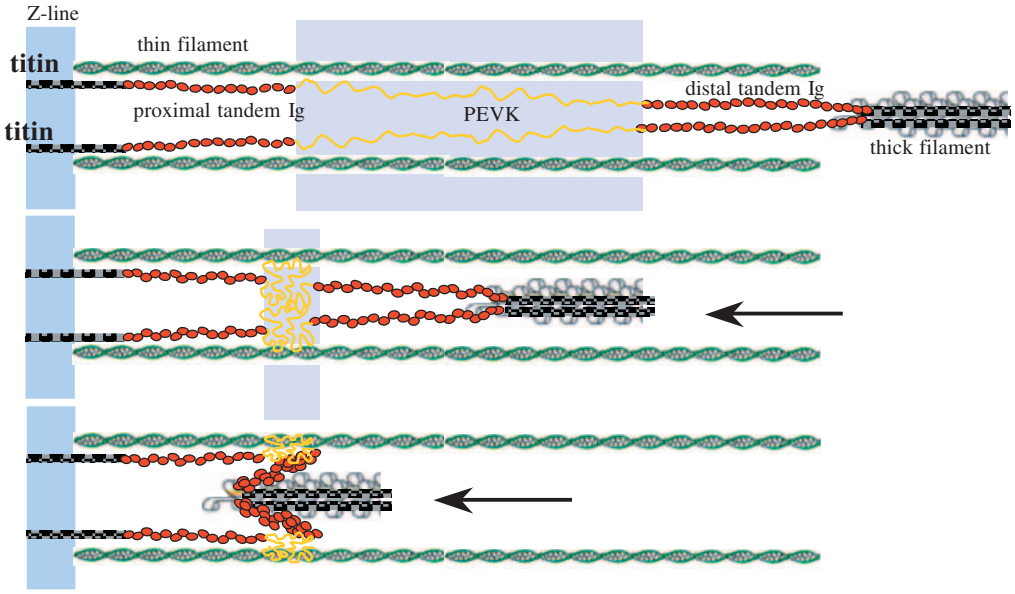

Fig. 7. Model of in situ PEVK-actin interaction in the sarcomere. Schematic arrangement of myofilaments in an extended and contracted sarcomere. Top panel, highly extended sarcomere. Middle panel, shortening sarcomere in which the PEVK domain is contracted. Bottom panel, shortening sarcomere in which the tip of the thick filament crossed the site of PEVK binding to the thin filament. The shaded area indicates the dimensions of the space occupied by the PEVK domain that defines the apparent concentration of the actin-binding sites in PEVK. As the dimensions of this space vary along the thin filament axis, the actin concentration is constant regardless of the size of the space. Arrows indicate the direction of movement during the contraction of a rather thick filament.

expressed various PEVK fragments: PPAK, polyE-rich and pure polyE.

Inhibition of in vitro motility by PEVK segments and fragments

In the presence of the different PEVK segments (Fig. 2A) and fragments (Fig. 4A), the in vitro acto-HMM motility was inhibited. In case of the contiguous PEVK segments, the greatest degree of motility inhibition was observed with PEVKII, the middle one third of the skeletal PEVK domain. In the case of PEVKIII, the C-terminal one third of PEVK, we observed a negligible reduction of motility. The findings suggest that the motility inhibitory effect of PEVK varies along its length. The inhibition of motility by PEVK derives from a mechanical interference rather than interfering with the chemomechanical transduction mechanisms. The differences in motility inhibition by the various PEVK segments are due to differences in the mechanical strength of the tether, which may themselves be caused by differences in the number of actin-PEVK bonds per PEVK segment, differences in the dissociation constants of the bonds, or both. The order of the apparent binding strength along the PEVK domain, based on the in vitro motility inhibitory effect is PEVKII>PEVKI>PEVKIII. The in vitro motility was also inhibited by the PEVK fragments at physiological ionic strength. The largest degree of motility inhibition was observed with the pure polyE fragment. Altogether the results suggest that local preponderance of polyE motifs conveys an enhanced local actin-binding property to PEVK.

Binding of F-actin and thin filaments by PEVK segments and fragments

The various PEVK segments and fragments were bound to F-actin in in vitro experiments. The relative binding strengths were established in ionic-strength dependent binding assays, in which the amount of F-actin attached to surface-immobilized PEVK was measured at various ionic strengths (Kellermayer and Granzier, 1996). Such assays have been used in the past to measure the binding between actin and titin fragments, and provides a semi-quantitative measure of the binding strength. The ionic strength dependence of PEVK-actin binding, also observed in previous works (Kulke et al., 2001; Yamasaki et al., 2001), indicates that the mechanism of the association between these two molecules is primarily electrostatic. Indeed, the motif structure of skeletal PEVK suggests the possibility of binding via electrostatic mechanisms (Greaser, 2001). The PEVK domain contains two major types of motif, the PPAK and polyE motifs, which alternate along its length (Greaser, 2001). The motifs have drastically different pI values: PPAK ~11 and polyE ~3. At physiological pH, the domains possess opposite charges, and the alternating positive and negative charges along the PEVK domain provide means for binding other muscle proteins or even neighboring PEVK domains (self-association). The PEVK domain is devoid of structural features of the actin-binding sites found in actin-binding proteins (Van Troys et al., 1999). Considering the previously suggested random, quasi-unfolded (Trombitás et al., 1998) or malleable (Ma and Wang, 2003) structure of PEVK, which lacks highly stable structural elements, the actin binding property of PEVK might be a general feature associated with a wider range of molecular elements rather than a local site.

The site of PEVK binding on actin is not precisely known. Here we have shown that the PEVK fragments bind to actin at sites that differ from the tropomyosin- and myosin-binding sites. Furthermore, the myofibril labeling experiments suggest that the site is also different from the site where nebulin associates with the actin filament. Although the PEVK-binding site on actin is not exactly established, the observation that the binding site is different from the site of association of the major sarcomeric actin-associated proteins indicates that PEVK binding to actin might be a physiologically relevant process.

The motif structure of skeletal PEVK (Fig. 1A) (Greaser, 2001) suggested that actin binding is related to the polyE motif, as the size and frequency of polyE motifs along skeletal PEVK

correlate with the actin-binding property: the largest size and highest frequency of polyE is found in the middle third, followed by the N-terminal third, then by the C-terminal third. In support of this, the largest degree of apparent actin binding was found with the pure polyE fragment. Although the nature of PEVK-actin interaction is primarily electrostatic, the exact binding mechanisms are, as yet, unclear. Most likely, multiple binding sites are involved and the accessibility of the sites is influenced by the dynamic structure of the PEVK domain.

Role and significance of PEVK-actin interaction in the muscle sarcomere

We have shown that fluorescently labeled PEVKII molecules bind to the thin-filament-containing I-band region of the skeletal muscle sarcomere. Thus, binding of PEVKII to actin probably occurs at sites different from the tropomyosin and nebulin binding sites, which are the major intrasarcomeric proteins along the thin filament (Clark et al., 2002). Our observation suggests that the entire I-band was labeled with the fluorescent PEVKII except for a short region near the AI junction. It is conceivable that in this region the actin filament is saturated with the in situ PEVK segment, and further PEVK fragment binding is not possible. The results nevertheless indicate that the thin filament is able to bind PEVK along its length, suggesting possible regulatory functions for the actin-PEVK interaction.

What could be a possible physiological role for PEVK-actin interaction? It has been shown earlier that the unloaded shortening of striated muscle is influenced by viscous and viscoelastic forces (de Tombe and ter Keurs, 1990; de Tombe and ter Keurs, 1991; de Tombe and ter Keurs, 1992). It has even been suggested that titin might play a role in influencing unloaded shortening velocity (Kulke et al., 2001; Opitz et al., 2003). We suggest a possible mechanism of how titin might inhibit unloaded sarcomere shortening (Fig. 7). As the sarcomere shortens, the actin-binding sites along PEVK become confined to a progressively smaller space, therefore their apparent concentration and hence the probability of PEVK-actin interaction increases. The apparent actin-binding site concentration depends strongly on the constrained diffusibility of the PEVK chain segments. The greatest apparent actin-binding site concentration is reached when the PEVK domain is fully contracted (i.e. at a sarcomere length of ~2 μm in soleus muscle) (Trombitás et al., 1998). Notably, the unloaded shortening velocity in various types of cardiac muscle has been previously shown to drop gradually below a sarcomere length of ~2 μm (de Tombe and ter Keurs, 1990; de Tombe and ter Keurs, 1991; de Tombe and ter Keurs, 1992). We speculate that the tip of the thick filament may travel past the PEVK domain if the PEVK remains associated with actin and the contraction is sufficiently rapid (Fig. 7, bottom panel). The association of the PEVK domain with the thin filament may inhibit further contraction in a similar manner to the inhibition of in vitro motility by imposing a viscous drag. The apparent drag coefficient depends on the lifetime of the PEVK-actin bond (Howard, 2001), which may be up to tens of seconds, estimated from the solid-state PEVK-actin binding assays. The greater the shortening velocity, the greater the viscous force generated. Eventually the viscous force relaxes on a timescale of the bond lifetime, owing to the rearrangement of the bonds. Furthermore, bond lifetime is reduced with external force (Bell, 1978; Evans and Ritchie, 1997). Thus, PEVK-actin interaction is likely to have only a transient effect on contraction, which may be manifested as a 'viscous bumper' function that slows down sarcomeric shortening before the boundary conditions (i.e., collision between the thick filament and the Z-line) are reached. Here we have also shown that different parts of the PEVK domain have different actin-binding properties: the greater the relative polyE motif content, the stronger the apparent actin binding. Different titin isoforms are expressed in different muscle types (Freiburg et al., 2000; Labeit and Kolmerer, 1995). The PEVK domain is differentially expressed via alternative splicing mechanisms: a short isoform is expressed in cardiac muscle, and long isoforms in the skeletal. By varying the relative polyE motif content of the expressed PEVK domain, the global actin-binding property of the PEVK domain, and hence its shortening modulatory function might be regulated.

This work was supported by grants from the Hungarian Science Foundation (OTKA T037935), Hungarian Ministry of Education (BIO-110/2002), European Union (HPRN-CT-2000-00091) and the South Trans-Danubian Co-operative Research Center to MSZK. MSZK is a Howard Hughes Medical Institute International Research Scholar. We thank Dr Siegfried Labeit for providing the human titin cDNA library, Emöke Bódis for providing tropomyosin, and Mihály Kovács, Béla Somogyi and Henk L. Granzier for their critical comments on the manuscript.

References

Bell, G. I. (1978). Models for the specific adhesion of cells to cells. *Science* **200**, 618-627.

Clark, K. A., McElhinny, A. S., Beckerle, M. C. and Gregorio, C. C. (2002). Striated muscle cytoarchitecture: an intricate web of form and function. *Annu. Rev. Cell Dev. Biol.* **18**, 637-706.

de Tombe, P. P. and ter Keurs, H. E. (1990). Force and velocity of sarcomere shortening in trabeculae from rat heart. Effects of temperature. *Circ. Res.* **66**, 1239-1254.

de Tombe, P. P. and ter Keurs, H. E. (1991). Sarcomere dynamics in cat cardiac trabeculae. *Circ. Res.* **68**, 588-596.

de Tombe, P. P. and ter Keurs, H. E. (1992). An internal viscous element limits unloaded velocity of sarcomere shortening in rat myocardium. *J. Physiol.* **454**, 619-642.

Evans, E. and Ritchie, K. (1997). Dynamic strength of molecular adhesion bonds. *Biophys. J.* **72**, 1541-1555.

Fabiato, A. (1988). Computer programs for calculating total from specified free or free from specified total ionic concentrations in aqueous solutions containing multiple metals and ligands. *Methods Enzymol.* **157**, 378-417.

Freiburg, A., Trombitas, K., Hell, W., Cazorla, O., Fougerousse, F., Centner, T., Kolmerer, B., Witt, C., Beckmann, J. S., Gregorio, C. C. et al. (2000). Series of exon-skipping events in the elastic spring region of titin as the structural basis for myofibrillar elastic diversity. *Circ. Res.* **86**, 1114-1121.

Fürst, D. O., Osborn, M., Nave, R. and Weber, K. (1988). The organization of titin filaments in the half-sarcomere revealed by monoclonal antibodies in immunoelectron microscopy: a map of ten nonrepetitive epitopes starting at the Z line extends close to the M line. *J. Cell Biol.* **106**, 1563-1572.

Gautel, M. and Goulding, D. (1996). A molecular map of titin/connectin elasticity reveals two different mechanisms acting in series. *FEBS Lett.* **385**, 11-14.

Granzier, H. L. and Labeit, S. (2004). The giant protein titin: a major player in myocardial mechanics, signaling, and disease. *Circ. Res.* **94**, 284-295.

Greaser, M. (2001). Identification of new repeating motifs in titin. *Proteins* **43**, 145-149.

Harada, Y., Noguchi, A., Kishino, A. and Yanagida, T. (1987). Sliding movement of single actin filaments on one-headed myosin filaments. *Nature* **326**, 805-808.

Helmes, M., Trombitas, K., Centner, T., Kellermayer, M., Labeit, S.,

Linke, W. A. and Granzier, H. (1999). Mechanically driven contour-length adjustment in rat cardiac titin's unique N2B sequence: titin is an adjustable spring. *Circ. Res.* **84**, 1339-1352.

Howard, J. (2001). *Mechanics of motor proteins and the cytoskeleton*. Sunderland, MA: Sinauer Associates.

Jin, J. P. (1995). Cloned rat cardiac titin class I and class II motifs. Expression, purification, characterization, and interaction with F-actin. *J. Biol. Chem.* **270**, 6908-6916.

Kellermayer, M. S. Z. (1997). Delayed dissociation of in vitro moving actin filaments from heavy meromyosin induced by low concentrations of Triton X-100. *Biophys. Chem.* **67**, 199-210.

Kellermayer, M. S. Z. and Granzier, H. L. (1996). Calcium-dependent inhibition of in vitro thin-filament motility by native titin. *FEBS Lett.* **380**, 281-286.

Kellermayer, M. S. Z., Hinds, T. R. and Pollack, G. H. (1995). Persisting *in vitro* motility of actin filaments at nanomolar ATP concentrations after ATP pretreatment. *Biochim. Biophys. Acta* **1229**, 89-95.

Knight, P. J. and Lovell, S. J. (1982). Preparation of native thin filaments. *Methods Enzymol.* **85**, 12-15.

Knight, P. J. and Trinick, J. A. (1982). Preparation of myofibrils. *Methods Enzymol.* **85**, 9-12.

Kron, S. J., Toyoshima, Y. Y., Uyeda, T. Q. and Spudich, J. A. (1991). Assays for actin sliding movement over myosin-coated surfaces. *Methods Enzymol.* **196**, 399-416.

Kulke, M., Fujita-Becker, S., Rostkova, E., Neagoe, C., Labeit, D., Manstein, D. J., Gautel, M. and Linke, W. A. (2001). Interaction between PEVK-titin and actin filaments: origin of a viscous force component in cardiac myofibrils. *Circ. Res.* **89**, 874-881.

Labeit, S. and Kolmerer, B. (1995). Titins: giant proteins in charge of muscle ultrastructure and elasticity. *Science* **270**, 293-296.

Laemmli, U. K. (1970). Cleavage of structural proteins during the assembly of the head of bacteriophage T4. *Nature* **227**, 680-685.

Linke, W. A., Ivemeyer, M., Olivieri, N., Kolmerer, B., Ruegg, J. C. and Labeit, S. (1996). Towards a molecular understanding of the elasticity of titin. *J. Mol. Biol.* **261**, 62-71.

Linke, W. A., Ivemeyer, M., Labeit, S., Hinssen, H., Ruegg, J. C. and Gautel, M. (1997). Actin-titin interaction in cardiac myofibrils: probing a physiological role. *Biophys. J.* **73**, 905-919.

Linke, W. A., Rudy, D. E., Centner, T., Gautel, M., Witt, C., Labeit, S. and Gregorio, C. C. (1999). I-band titin in cardiac muscle is a three-element molecular spring and is critical for maintaining thin filament structure. *J. Cell Biol.* **146**, 631-644.

Linke, W. A., Kulke, M., Li, H., Fujita-Becker, S., Neagoe, C., Manstein, D. J., Gautel, M. and Fernandez, J. M. (2002). PEVK Domain of titin: an entropic spring with actin-binding properties. *J. Struct. Biol.* **137**, 194-205.

Ma, K. and Wang, K. (2003). Malleable conformation of the elastic PEVK segment of titin: non-cooperative interconversion of polyproline II helix, beta turn and unordered structures. *Biochem. J.* **374**, 687-695.

Ma, K., Kan, L. and Wang, K. (2001). Polyproline II helix is a key structural motif of the elastic PEVK segment of titin. *Biochemistry* **40**, 3427-3438.

Margossian, S. S. and Lowey, S. (1982). Preparation of myosin and its subfragments from rabbit skeletal muscle. *Methods Enzymol.* **85**, 55-72.

Maruyama, K. (1997). Connectin/titin, giant elastic protein of muscle. *FASEB J.* **11**, 341-345.

Maruyama, K., Hu, D. H., Suzuki, T. and Kimura, S. (1987). Binding of actin filaments to connectin. *J. Biochem.* **101**, 1339-1346.

Miller, M. K., Granzier, H., Ehler, E. and Gregorio, C. C. (2004). The sensitive giant: the role of titin-based stretch sensing complexes in the heart. *Trends Cell Biol.* **14**, 119-126.

Opitz, C. A., Kulke, M., Leake, M. C., Neagoe, C., Hinssen, H., Hajjar, R. J. and Linke, W. A. (2003). Damped elastic recoil of the titin spring in myofibrils of human myocardium. *Proc. Natl. Acad. Sci. USA* **100**, 12688-12693.

Pardee, J. D. and Spudich, J. A. (1982). Purification of muscle actin. *Methods Enzymol.* **85**, 164-182.

Soteriou, A., Gamage, M. and Trinick, J. (1993). A survey of interactions made by the giant protein titin. *J. Cell Sci.* **104**, 119-123.

Trombitás, K. and Granzier, H. (1997). Actin removal from cardiac myocytes shows that near Z line titin attaches to actin while under tension. *Am. J. Physiol.* **273**, C662-C670.

Trombitás, K., Greaser, M., Labeit, S., Jin, J. P., Kellermayer, M., Helmes, M. and Granzier, H. (1998). Titin extensibility in situ: entropic elasticity of permanently folded and permanently unfolded molecular segments. *J. Cell Biol.* **140**, 853-859.

Tskhovrebova, L. and Trinick, J. (2003). Titin: properties and family relationships. *Nat. Rev. Mol. Cell Biol.* **4**, 679-689.

Van Troys, M., Vandekerckhove, J. and Ampe, C. (1999). Structural modules in actin-binding proteins: towards a new classification. *Biochim. Biophys. Acta* **1448**, 323-348.

Wang, K., McClure, J. and Tu, A. (1979). Titin: major myofibrillar components of striated muscle. *Proc. Natl. Acad. Sci. USA* **76**, 3698-3702.

Yamasaki, R., Berri, M., Wu, Y., Trombitas, K., McNabb, M., Kellermayer, M. S., Witt, C., Labeit, D., Labeit, S., Greaser, M. et al. (2001). Titin-actin interaction in mouse myocardium: passive tension modulation and its regulation by calcium/S100A1. *Biophys. J.* **81**, 2297-2313.